

Accelerating iterative linear equation solver using modified domain-wall fermion matrix in lattice QCD simulations

Wei-Lun Chen¹[0000-0002-8542-9126], Issaku Kanamori²[0000-0003-4467-1052],
Hideo Matsufuru³[0000-0003-1056-3969], and Hartmut Neff⁴

¹ Particle and Nuclear Physics, Graduate Institute for Advanced Studies, Graduate University for Advanced Studies (SOKENDAI), Oho 1-1, Tsukuba 305-0801, Japan
wlchen@post.kek.jp

² RIKEN Center for Computational Science 7-1-26 Minatojima-minami-machi, Chuo-ku Kobe, Hyogo 650-0047, Japan kanamori-i@riken.jp

³ Computing Research Center, High Energy Accelerator Research Organization (KEK) and Accelerator Science Program, Graduate University for Advanced Studies (SOKENDAI), Oho 1-1, Tsukuba 305-0801, Japan hideo.matsufuru@kek.jp

⁴ Luzernerstrasse 43, 6330, Switzerland hartmutneff@aol.com

Abstract. Lattice simulations of Quantum Chromodynamics (QCD) enable one to calculate the low-energy properties of the strong interaction among quarks and gluons based on the first principle. The most time-consuming part of the numerical simulations of lattice QCD is typically solving a linear equation for the quark matrix. In particular, a discretized quark formulation called the domain-wall fermion operator requires a high numerical cost, while retaining the lattice version of the chiral symmetry to good precision. The domain-wall operator is defined on a five-dimensional (5D) space extending the four-dimensional (4D) spacetime with an extra fifth coordinate. After solving the linear equation in 5D space, the result vector is projected onto the original 4D space. There is a variant of the domain-wall operator that improves the convergence of the 5D linear equation while unchanging the 4D solution vector. In this paper, we examine how this variant of the domain-wall operator accelerates the iterative linear equation solver in practical setups. We also measure the eigenvalues of the operator and compare the condition number with the convergence of the solver. We use a generic lattice QCD code set Bridge++ that is planned to be released including the improved form of the domain-wall operator examined in this work with code for the GPU.

Keywords: lattice QCD · iterative linear equation solver · high performance computing

1 Introduction

Large-scale simulations of lattice Quantum Chromodynamics (QCD) have been a challenge for the high-performance computing for a long time. The QCD is the

fundamental theory of the strong interaction among quarks and gluons, which is formulated based on the invariance under the local $SU(3)$ gauge transformation on the color degree of freedom of the quark and gluon fields. While the fundamental theory is known, it is quite difficult to solve it analytically because of the strong coupling of this theory. The lattice QCD is a field theory formulated on the Euclidean discretized spacetime. Employing the path integral quantization, this theory enables numerical evaluation of the physical quantities using the Monte Carlo algorithms. Thus, the lattice QCD simulations provide a general procedure to investigate QCD based on the first principle. Such a calculation is particularly important in the search for phenomena beyond the standard model through precision evaluation of the hadronic scattering processes. Lattice QCD is also important in the quantitative understanding of the nuclear force among hadrons, the phase structure of QCD at finite temperature and density, and so on.

The most time-consuming part of the lattice QCD simulation is solving a linear equation for the quark (fermion) matrix, which is typically large-scale, sparse, and solved by iterative methods. There is a variety in the form of the fermion matrix since the only required condition is that it approaches QCD in the continuum limit. In this paper, we focus on the type of matrix called the domain-wall fermion operator. This fermion matrix has an important feature that preserves the chiral symmetry, an important symmetry of QCD, on the lattice with good precision. The domain-wall operator is defined in the five-dimensional (5D) space, which extends the four-dimensional (4D) spacetime by adding the fifth coordinate. The physical modes in the original four-dimensional space are picked up from the two edges in the fifth direction. Since the domain-wall fermion matrix is defined in the five-dimensional space, the numerical cost is higher than that of other formulations. Thus improving the convergence of the fermion matrix solver is a quite important subject in the numerical simulations.

One of the authors (H. Neff) proposed a form of domain-wall operator that improves the convergence of the solver while unchanging the physical modes in the four-dimensional space [16]. This paper aims at a systematic and practical investigation of Neff's form and how it improves the convergence of the solver. While Ref. [16] already examined the effect of the improved form on several parameter sets, we add several new setups including the operator with the link smearing. We determine the condition number of the matrix by measuring the lowest and highest eigenvalues of the Hermitian domain-wall matrix and compare with the convergence of the Conjugate Gradient (CG) solver. In the numerical study, we employ the Bridge++ code set [1] with an extension to incorporate Neff's improved form of the domain-wall matrix. We use the code for GPU implemented with OpenACC [7].

This paper is organized as follows. The next section introduces the lattice QCD and our target fermion matrix in a certain depth. While the equations necessary to implement the fermion matrix used in this work are displayed to make the description self-contained, the essential ingredient is the introduction of a tunable parameter α in the 5D matrix that does not change the 4D solution

vector. Section 3 shows our numerical results. We examine the effect of α in the modified matrix on the convergence of CG solver. The last section is devoted to our conclusion and outlook.

2 Lattice QCD

2.1 Lattice QCD and chiral symmetry

The lattice QCD action in four-dimensional Euclidean space is written as follows:

$$S_{\text{QCD}} = \sum_x \{ (S_G[U_\mu(x)] + \bar{\psi}(x) D_F[U] \psi(x)) \}, \quad (1)$$

where S_G is a gauge action, $\psi(x)$ and $\bar{\psi}(x)$ anti-commuting Grassmann fields representing quark and anti-quark, $D_F[U]$ a fermion operator depending on the link variable $U_\mu(x)$, $x = (x_1, x_2, x_3, x_4)$ a lattice site, where the lattice spacing a is set to unity for simplicity. $U_\mu(x)$ is a 3×3 complex matrix field representing the gauge field. ψ has the color and spinor degrees of freedom in addition to the lattice site x . The spinor has 4 components that represent the up and down spin for quark and anti-quark. Thus the quark field has $3 \times 4 = 12$ complex components on each site x .

Employing the path integral quantization, the QCD partition function reads

$$\begin{aligned} & \int \mathcal{D}U \mathcal{D}\psi \mathcal{D}\bar{\psi} \exp \left[-S_G - \sum_x \bar{\psi}(x) D_F[U] \psi(x) \right] = \int \mathcal{D}U \det(D_F) e^{-S_G} \\ & = \int \mathcal{D}U \mathcal{D}\phi \mathcal{D}\phi^\dagger \exp \left[-S_G - \frac{1}{2} \sum_x \phi^\dagger(x) D_F[U]^{-1} \phi(x) \right], \end{aligned} \quad (2)$$

where complex (ordinary number) field $\phi(x)$ is introduced as Gaussian integration variables. Applying a Monte Carlo method, the expectation value of a physical observable \mathcal{O} is represented as

$$\langle \mathcal{O}[U, \psi, \bar{\psi}] \rangle = \frac{1}{N} \sum_i^N \mathcal{O}[U^{(i)}, S_q^{(i)}]. \quad (3)$$

Here, the gauge field configurations $\{U^{(i)}\}$ are assumed to be generated with the Boltzmann weight $\exp[-S_G] \det(D_F)$, and $S_q^{(i)}$ is a quark propagator obtained by solving a linear equation for the fermion matrix D_F ,

$$D_F[U^{(i)}]_{y,x} S_q^{(i)}(x) = b_y, \quad (4)$$

where the color and spinor indices are omitted for simplicity. To obtain the physical quantities with high precision, one needs to solve this linear equation many times to calculate $\mathcal{O}[U^{(i)}, S_q^{(i)}]$ as well as during the generation of the gauge configurations. Thus solving this linear equation is a typical bottleneck of lattice QCD simulations.

In discretizing the continuum QCD action, there is a variation of the action on the lattice, since the only required condition is that the lattice action approaches to the QCD action in the continuum limit, $a \rightarrow 0$, where a is the lattice spacing. Thus a number of lattice actions have been proposed intending a rapid approach to the continuum limit. Each lattice fermion action has its own pros and cons. One of the most popular fermion operators is the Wilson fermion,

$$D_W(x, y; M) = (4 + M)\delta_{x,y} - \frac{1}{2} \sum_{\mu=1}^4 \left\{ (1 - \gamma_\mu)U_\mu(x)\delta_{x+\hat{\mu},y} + (1 + \gamma_\mu)U_\mu^\dagger(x - \hat{\mu})\delta_{x-\hat{\mu},y} \right\}, \quad (5)$$

where M is quark mass, $\hat{\mu}$ is a unit vector in μ -th direction ($\mu = 1, 2, 3, 4$), γ_μ is a 4×4 complex matrix acting on the spinor components. The improved form of the Wilson fermion action, called clover fermion, is extensively used in large-scale simulations of lattice QCD. It has a disadvantage, however, that a symmetry called chiral symmetry, which is satisfied by the QCD action for vanishing quark mass, is explicitly violated even with setting $M = 0$.

In the continuum QCD, the chiral symmetry is represented as

$$\gamma_5 D_F + D_F \gamma_5 = 0, \quad (6)$$

where $\gamma_5 = \gamma_1 \gamma_2 \gamma_3 \gamma_4$. This symmetry concerns the left- and right-handed components of the quark field. The spontaneous breakdown of this symmetry at low-energy ensures the smallness of the pion masses and is attributed to most of the masses of the proton and the neutron. The chiral symmetry is also the basis of the phenomenological properties of the hadrons. Thus the quark action that respects the chiral symmetry has particular importance in understanding the chiral dynamics of QCD. For the Wilson fermion action, the chiral symmetry is restored only in the continuum limit.

On the lattice, the chiral symmetry had been a difficulty for a long time. Understanding of the chiral symmetry on the lattice was proceeded by the discovery of the Ginsparg-Wilson relation [11],

$$\gamma_5 D_F + D_F \gamma_5 = a D_F R \gamma_5 D_F, \quad (7)$$

where R is a certain constant. [12, 14]. After the realization of the Ginsparg-Wilson relation as the exact chiral symmetry on the lattice, several fermion actions that satisfies the Ginsparg-Wilson relation exactly or approximately have been proposed. The Domain-wall fermion is the latter kind of formulation and in the limit of the infinite extent of the fifth direction, $L_s \rightarrow \infty$, it satisfies the Ginsparg-Wilson relation exactly.

2.2 Domain-wall fermion matrix

The domain-wall fermion was proposed by Kaplan [13] intending to formulate the chiral gauge theory. The domain-wall fermion is defined on the five-dimensional

space by adding fifth coordinate to the four-dimensional spacetime, and a large negative mass is introduced to the Wilson operator kernel (5). The light modes appear on the two edges in the fifth direction. After the realization of the domain-wall fermion as a light fermion formulation [17, 10], several improved forms have been proposed [3, 6, 8]. These variants are described by the following form [6]:

$$D_{DW} = \begin{pmatrix} D_+^{(1)} & D_-^{(1)}P_- & 0 & \cdots & 0 & -mD_-^{(1)}P_+ \\ D_-^{(2)}P_+ & D_+^{(2)} & D_-^{(2)}P_- & & & 0 \\ 0 & D_-^{(3)}P_+ & D_+^{(3)} & D_-^{(3)}P_- & & 0 \\ \vdots & & \ddots & \ddots & \ddots & \vdots \\ 0 & & & D_-^{(L_s-1)}P_+ & D_+^{(L_s-1)} & D_-^{(L_s-1)}P_- \\ -mD_-^{(L_s)}P_- & 0 & \cdots & 0 & D_-^{(L_s)}P_+ & D_+^{(L_s)} \end{pmatrix} \quad (8)$$

where m is quark mass, $P_- = (1 - \gamma_5)/2$, $P_+ = (1 + \gamma_5)/2$,

$$D_+^{(i)} = b_i D_W + 1, \quad D_-^{(i)} = c_i D_W - 1, \quad (9)$$

$D_W = D_W(-M_0)$ is the Wilson operator (5) with large negative mass $-M_0$, where $M_0 = O(1)$ is called the domain-wall height. There are several choices for the parameters b_i and c_i : $(b_i, c_i) = (1, 0)$ [17, 10], $(b_i, c_i) = (1, 1)$ [3], $b_i - c_i = \text{const.}$ (independent of i) called the Möbius fermion [6], and $b_i = c_i$ chosen depending on i so as to optimize the Ginsparg-Wilson relation [8]. In this paper we only examine the cases (b_i, c_i) independent of i .

In the fifth direction, the following boundary condition is imposed at $s = 1$ and L_s :

$$P_+ \psi(s=0) = P_- \psi(s=L_s+1) = 0. \quad (10)$$

The fermion field in four-dimensional space is given as⁵

$$\begin{aligned} q(x) &= P_- \psi(x, s=1) + P_+ \psi(x, s=L_s), \\ \bar{q}(x) &= \bar{\psi}(x, s=1)(-D_-^{(1)})P_+ + \bar{\psi}(x, s=L_s)(-D_-^{(L_s)})P_-. \end{aligned} \quad (11)$$

In the limit of $L_s \rightarrow \infty$, the lattice chiral symmetry is satisfied exactly. This limit corresponds to the overlap fermion operator, $D_{\text{ov}} = 1 + \gamma_5 \text{sign}(\gamma_5 D_W)$ in the massless case, which practically requires large numerical resources.

Link smearing Currently the link smearing is frequently adopted as an improvement procedure for fermion actions. The link smearing is essentially the integration of the surrounding gauge field into the link variable, $U_\mu(x)$. We consider the stout projection combined with the APE smearing [15]:

$$\begin{aligned} C_\mu(x) &= \sum_{\nu \neq \mu} \rho [U_\nu(x)U_\mu(x+\hat{\nu})U_\nu^\dagger(x+\hat{\mu}) + U_\nu^\dagger(x-\hat{\nu})U_\mu(x-\hat{\nu})U_\nu(x-\hat{\nu}+\hat{\mu})], \\ U_\mu(x)' &= \exp([C_\mu(x)U_\mu^\dagger(x)]_{\text{AT}}) U_\mu(x), \end{aligned} \quad (12)$$

⁵ This definition of $\bar{q}(x)$ corresponds to \tilde{q}_x called “traditional choice” in Ref. [5].

where $[\dots]_{\text{AT}}$ represents anti-Hermitian and traceless operation, and ρ is a tunable parameter. This smearing step (12) can be repeatedly applied. The fermion operator can be improved by adopting the smeared link variable instead of the original one.

2.3 Better conditioned form of domain-Wall operator

Improved form of the domain-wall fermion operator which unchanges the four-dimensional fermion field was proposed by H. Neff [16]. This form is represented as follows.

$$D_{DW}^{(\alpha)} = \begin{pmatrix} D_+^{(1)}(P_- + \alpha P_+) & \alpha D_-^{(1)} P_- & 0 & \cdots & -m D_-^{(1)} P_+ \\ \alpha D_-^{(2)} P_+ & \alpha D_+^{(2)} & \alpha D_-^{(2)} P_- & & 0 \\ \vdots & \ddots & \ddots & \ddots & \vdots \\ -m D_-^{(L_s)} P_- & 0 & \cdots & \alpha D_-^{(L_s)} P_+ & D_+^{(L_s)}(P_+ + \alpha P_-) \end{pmatrix} \quad (13)$$

Note that except for the four corners of the fifth coordinate matrix, each four-dimensional block is multiplied by α . The top-left and bottom-right blocks are modified by multiplying by $(P_{\mp} + \alpha P_{\pm})$, respectively, and the top-right and bottom-left blocks are unchanged. This modification does not change the four-dimensional quark field, while it affects the convergence of the linear equation in five-dimensional space.

There is a relation between $D_{DW}^{(\alpha)}$ and $D_{DW} = D_{DW}^{(\alpha=1)}$ that

$$D_{DW}^{(\alpha)} \mathcal{P} = D_{DW}^{(\alpha=1)} \mathcal{P} \mathcal{A}, \quad (14)$$

where

$$\mathcal{P} = \begin{pmatrix} P_- & P_+ & 0 & \cdots & 0 \\ 0 & P_- & P_+ & \ddots & \vdots \\ \vdots & \ddots & \ddots & \ddots & 0 \\ 0 & \ddots & P_- & P_+ & \\ P_+ & 0 & \cdots & 0 & P_- \end{pmatrix}, \quad \mathcal{A} = \begin{pmatrix} 1 & 0 & \cdots & 0 \\ 0 & \alpha & & \vdots \\ \vdots & \ddots & \ddots & \vdots \\ \vdots & & \ddots & \alpha & 0 \\ 0 & \cdots & \cdots & 0 & \alpha \end{pmatrix}. \quad (15)$$

We need to solve a 5D equation

$$D_{DW}^{(\alpha=1)} x_5 = b_5, \quad (16)$$

where according to Eq. (11) $b_5 = (-D_-) \mathcal{P}^\dagger(0, \dots, 0, b_4)^T$ for a 4D source vector b_4 , with $D_- = \text{diag}(D_-^{(1)}, \dots, D_-^{(L_s)})$. Once a 5D solution vector x_5 is determined, the 4D solution vector x_4 is provided as $x_4 = [\mathcal{P}^\dagger x_5]_{s=1}$. Due to the relation (14), the solution of $D_{DW}^{(\alpha)} x_5^{(\alpha)} = b_5$ give the same 4D solution x_4 , since

$$\mathcal{P}^\dagger x_5 = (D_{DW} \mathcal{P})^{-1} b_5 = (D_{DW}^{(\alpha)} \mathcal{P} \mathcal{A}^{-1})^{-1} b_5 = \mathcal{A} \mathcal{P}^\dagger (D_{DW}^{(\alpha)})^{-1} b_5 = \mathcal{A} \mathcal{P}^\dagger x_5^{(\alpha)}, \quad (17)$$

where $\mathcal{P}^\dagger = \mathcal{P}^{-1}$, and $[\mathcal{A} \mathcal{P}^\dagger x_5^{(\alpha)}]_{s=1} = [\mathcal{P}^\dagger x_5^{(\alpha)}]_{s=1}$. Thus if the linear equation with $\alpha \neq 1$ can be solved faster than the original equation (16), the numerical cost would be reduced.

Even-odd preconditioning Noting that the D_W and D_{DW} contain nearest neighbor coupling, by dividing sites into even and odd sites, $D_{DW}x = b$ is represented as

$$D_{DW}x = \begin{pmatrix} D_{ee} & D_{eo} \\ D_{oe} & D_{oo} \end{pmatrix} \begin{pmatrix} x_e \\ x_o \end{pmatrix} = \begin{pmatrix} b_e \\ b_o \end{pmatrix} = b. \quad (18)$$

One arrives at the even-odd preconditioned linear equation,

$$Dx_e \equiv (1 - D_{ee}^{-1}D_{eo}D_{oo}^{-1}D_{oe})x_e = \tilde{b}_e, \quad (19)$$

$$\tilde{b}_e = D_{ee}^{-1}(b_e - D_{eo}D_{oo}^{-1}b_o), \quad (20)$$

$$x_o = D_{oo}^{-1}(b_o - D_{oe}x_e). \quad (21)$$

One needs to solve Eq. (19) whose matrix D usually has a smaller condition number than D_{DW} . There are two ways to divide the sites into even and odd: in the five-dimensional space or the four-dimensional space. We adopt the latter for simplicity and similarity with other fermion formulations. In this paper we focus on the effect of α on the convergence of the iterative solver, and do not concern the details of implementation and its performance which is described in [7].

Note that there is another version of even-odd preconditioned equation,

$$(1 - D_{eo}D_{oo}^{-1}D_{oe}D_{ee}^{-1})y_e = b'_e, \quad (22)$$

where $b'_e = b_e - D_{eo}D_{oo}^{-1}b_o$ and $x_e = D_{ee}^{-1}y_e$. However, the relation (14) means $D_{DW}^{(\alpha)} = D_{DW}(\mathcal{P}\mathcal{A}^{-1}\mathcal{P}^\dagger)$, and thus $D_{ee}^{(\alpha)} = D_{ee}^{(\alpha=1)}(\mathcal{P}\mathcal{A}^{-1}\mathcal{P}^\dagger)$ and so on. In Eq. (22), $(\mathcal{P}\mathcal{A}^{-1}\mathcal{P}^\dagger)$ and $(\mathcal{P}\mathcal{A}^{-1}\mathcal{P}^\dagger)^{-1} = \mathcal{P}\mathcal{A}\mathcal{P}^\dagger$ cancel each other, which results in no effect on the convergence of the solver.

In lattice QCD simulations, the BiCGStab algorithm is often a good choice. However, for the domain-wall fermion matrix, BiCGStab does not converge. This is because the eigenvalues of D_{DW} distribute in the negative real part. Thus the CG algorithm for $D^\dagger D$ is applied, where “ \dagger ” denotes Hermitian conjugate, *i.e.*, taking the complex conjugate and the transpose of the matrix D in Eq. (19).

It is well-known that a single precision solver can work as a preconditioner in the solver in double precision which is the precision practically required in numerical simulations. In such a multi-precision solver, most of the time is consumed in the single precision solver, and hence the performance of matrix multiplication to a vector in single precision determines the efficiency of solver algorithms. It is also expected that the convergence property of the iterative solver does not differ much for double and single precision. Thus in the following we show the convergence of the solver for the single precision solver only.

3 Results

3.1 Numerical setup

We perform a numerical experiment to investigate how the introduction of the parameter α improves the convergence of five-dimensional solver. For practical

investigation, we generate three ensembles of gauge configuration generated with quenched approximation, namely, without the quark vacuum polarization effect. They are generated with the plaquette gauge action at the gauge coupling $\beta = 6.0$ and 5.7 , which roughly correspond to the values of lattice spacing $a \simeq 0.1$ and 0.2 fm, respectively. For $\beta = 6.0$, two lattice volumes 16^4 and 32^4 are adopted. For the $\beta = 5.7$, we generate a 16^4 lattice that roughly corresponds to the same physical volume as the 32^4 lattice with $\beta = 6.0$. On these configurations, the parameter of the domain-wall operator $M_0 = 1.8$ is used as a typical value in practical simulations, as adopted by the RBC/UKQCD Collaboration [2].

To examine the effect of the link smearing, we apply three steps of the stout projection [15] with the APE smearing with $\rho = 0.1$ to the $\beta = 6.0$ configurations. This corresponds to the setup adopted by the JLQCD collaboration [9]. In this case, $M_0 = 1.0$ is adopted since the lattice artifact to shift the best value of M_0 from 1 due to the interaction is largely suppressed.

On these ensembles, the parameters $(b, c) = (1.5, 0.5)$ and $(1.0, 1.0)$ are adopted with two values of $L_s = 8$ and 16 . The values of parameters $(b, c) = (1.5, 0.5)$ are adopted by JLQCD Collaboration [9] and RBC/UKQCD Collaboration [2], and $(b, c) = (1.0, 1.0)$ corresponds to the Borici's form [3]. We observe the convergence of the CG solver for several values of quark mass in the range of $m = 0.001$ – 0.01 , with varying the value of α .

As the simulation code, we employ the Bridge++ code set [4, 1] with an extension to offloading code for the GPU implemented using OpenACC [7]. The numerical computation is done on the Pegasus system at University of Tsukuba, whose each node is composed of Intel Xeon processor and a single NVIDIA H100 GPU. All the computation is performed on a single process with single GPU device. Since this work concerns the algorithmic convergence of an iterative solver, we do not discuss the performance of the code which is described in [7].

3.2 Result for $\beta = 6.0$ on the 16^4 lattice

Let us start with examining the effect of α on the convergence of CG solver on the 16^4 lattice generated with the gauge coupling $\beta = 6.0$. In the unsmearred cases, we set $M_0 = 1.8$ as aforementioned. The CGNR solver is applied in single precision with the convergence criterion $|r|^2 < 10^{-14}$.

Figure 1 shows the convergence iteration number against α on a single configuration without the link smearing. Fluctuation against the gauge configuration will be discussed later. The top panels of Fig. 1 display the result for $(b, c) = (1.5, 0.5)$ with $L_s = 8$ and 16 . For $L_s = 8$, $\alpha \simeq 0.6$ most improves the convergence, and 25% improvement compared to $\alpha = 1$ independently of the quark mass. While $L_s = 16$ requires slightly more iterations until convergence, the result shows the same tendency that $\alpha \simeq 0.5$ is the best, while the improvement decreases as the quark mass from 25% for $m = 0.001$ to 20% for $m = 0.01$.

The bottom panels of Figure 1 display the result for $b = 1.0$, $c = 1.0$ (Borici's setting). For both the $L_s = 8$ and 16 , $\alpha \simeq 0.5$ improves the convergence most, for which about 36% acceleration is achieved independently of the quark mass

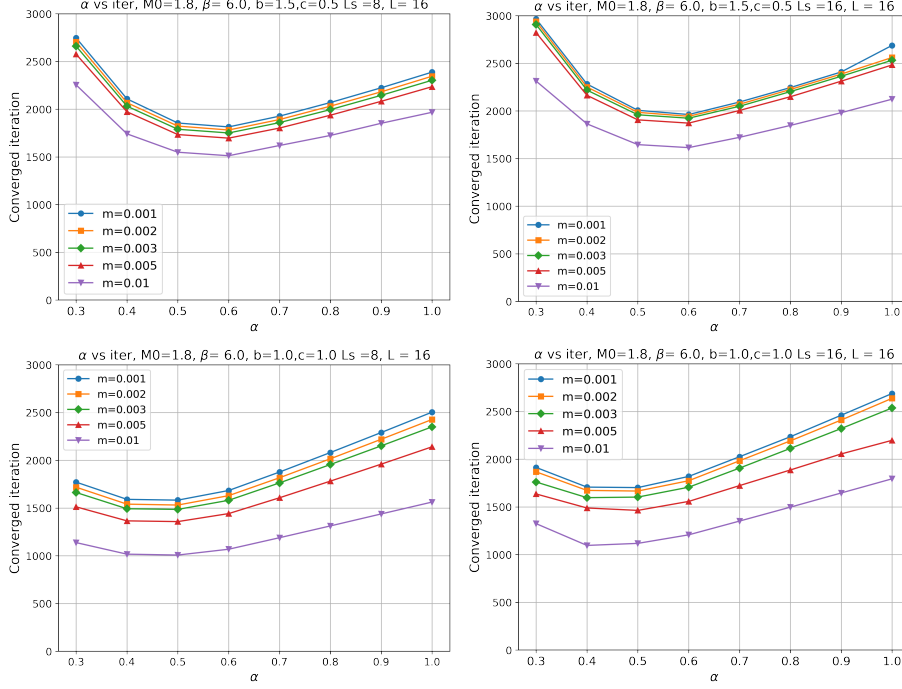


Fig. 1. Converged number of CG iteration for $\beta = 6.0$ on $(L = 16)^4$ lattice, $M_0 = 1.8$ (without smearing), $(b, c) = (1.5, 0.5)$ (top panels) $L_s = 8$ (left) and 16 (right) and $(b, c) = (1.0, 1.0)$ (bottom panels).

and L_s . As an observation, the quark mass dependence of converged iteration is larger than the case of $(b, c) = (1.5, 0.5)$.

Next, we observe the effect of the link smearing. For the domain-wall operator with smeared link, we set $M_0 = 1.0$. The top panels of Figure 2 show the result for $b = 1.5, c = 0.5$. Together with the link smearing, this choice of the parameters corresponds to the setup adopted by the JLQCD Collaboration, except that the configuration in this work is in the quenched approximation. Around $\alpha \simeq 0.5$, the converged number of CG iterations becomes minimum where 37% acceleration is achieved for $m = 0.001$. We find that changing L_s does not affect the optimal value of α , and has only little effect on the iteration number for the convergence.

The bottom panels of Figure 2 shows the result for $(b, c) = (1.0, 1.0)$. A similar tendency to the $(b, c) = (1.5, 0.5)$ case is found while the best value of α becomes around 0.4. The achieved speed-up is about 40 % for $m = 0.001$. Also small effect of L_s on the convergence is observed.

Condition number The convergence of the CG algorithm is represented by the condition number which is defined as the ratio of the maximum and minimum eigenvalues of the matrix. We measure the minimum and maximum eigenvalues

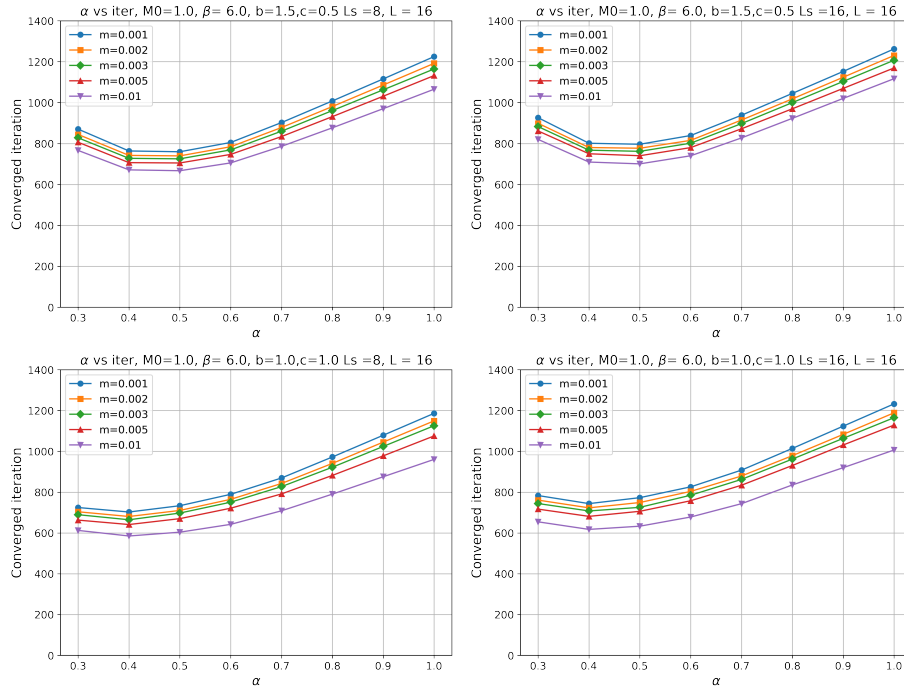


Fig. 2. Converged number of CG iteration for $\beta = 6.0$ on $(L = 16)^4$ lattice, $M_0 = 1.0$ (with smearing), $(b, c) = (1.5, 0.5)$ (top panels) $L_s = 8$ (left) and 16 (right) and $(b, c) = (1.0, 1.0)$ (bottom panels).

of $D^\dagger D$ by applying the implicitly restarted Lanczos algorithm in the double precision which is implemented in the Bridge++ code.

In Figure 3, the measured condition number against the value of α is displayed for the domain-wall operators without the link smearing. We display the result for $(b, c) = (1.5, 0.5)$ (top panels) and $(b, c) = (1.0, 1.0)$ (bottom) for $m = 0.001$. The left panels show the values of the computed condition number on three configurations. While the fluctuation of the condition number against configuration is substantial, as displayed in the right panels of Figure 3, normalizing by the values at $\alpha = 1$, the effect of α itself is stable. The α dependence of the condition number exhibits similar behavior to the converged number of iterations shown in Figure 1, which is consistent with the theoretical expectation.

Figure 4 shows the condition numbers and those normalized by the values at $\alpha = 1.0$. Similarly to the case without smearing, the behavior of the condition numbers is consistent with the converged number of CG iterations in Fig. 4. It is also observed that the fluctuation against the configuration is absorbed by normalizing with the values at $\alpha = 1$.

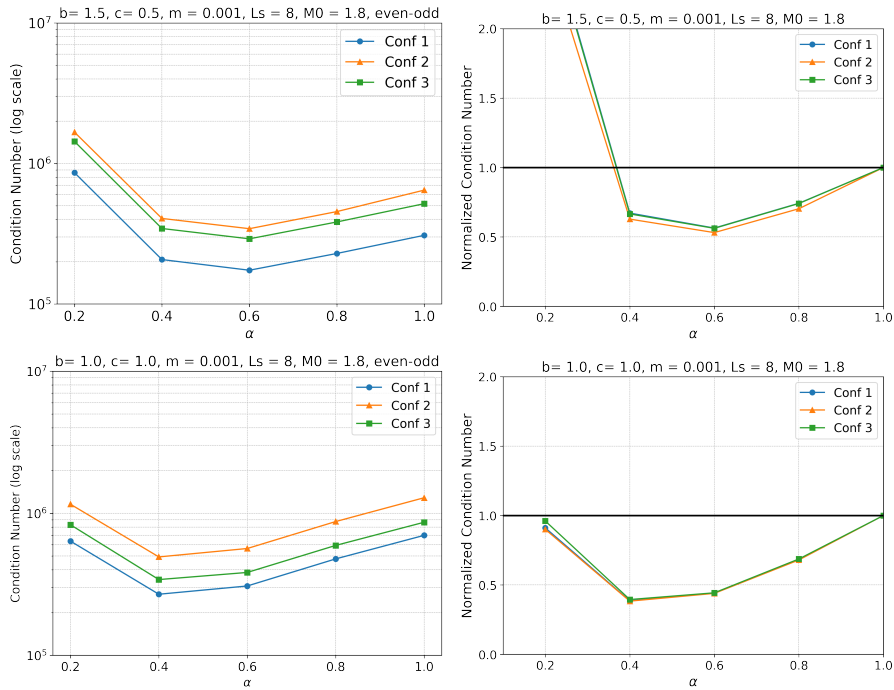


Fig. 3. Result of the condition number on the 16^4 lattice at $\beta = 6.0$ for the domain-wall operator without link smearing with parameters $M_0 = 1.8$, $(b, c) = (1.5, 0.5)$ (top panels) and $(1.0, 1.0)$ (bottom), $m = 0.001$. The left panels show the observed condition number on three configurations. The right panels show the condition numbers normalized by the values for $\alpha = 1$.

3.3 Result for $\beta = 6.0$ on the 32^4 lattice

To examine the effect of lattice volume on the convergence of the CG algorithm, we measure the converged iteration number against α on a 32^4 lattice with configurations generated at the gauge coupling $\beta = 6.0$. This means that the lattice volume is doubled in each direction compared to the lattice examined in the previous subsection. On this lattice size, we only show the results for $L_s = 8$.

Figure 5 shows the results of the converged number of CG iterations for unsmearing and smeared cases with $(b, c) = (1.5, 0.5)$ and $(1.0, 1.0)$. The acceleration of CG convergence for $m = 0.001$, the severest one of the measured quark mass, is in the range of 24% (top-left panel)–40% (bottom-left).

As a different feature from the results on 16^4 lattice in Figs 1 and 2, large dependence on the quark mass is observed. This is considered that 16^4 lattice may be affected by finite volume effect, since for the present small values of quark mass, the lattice size of about 1.6 fm is not sufficiently larger than the pion Compton wavelength. This should be examined by observing the pion spectrum by varying the lattice volume.

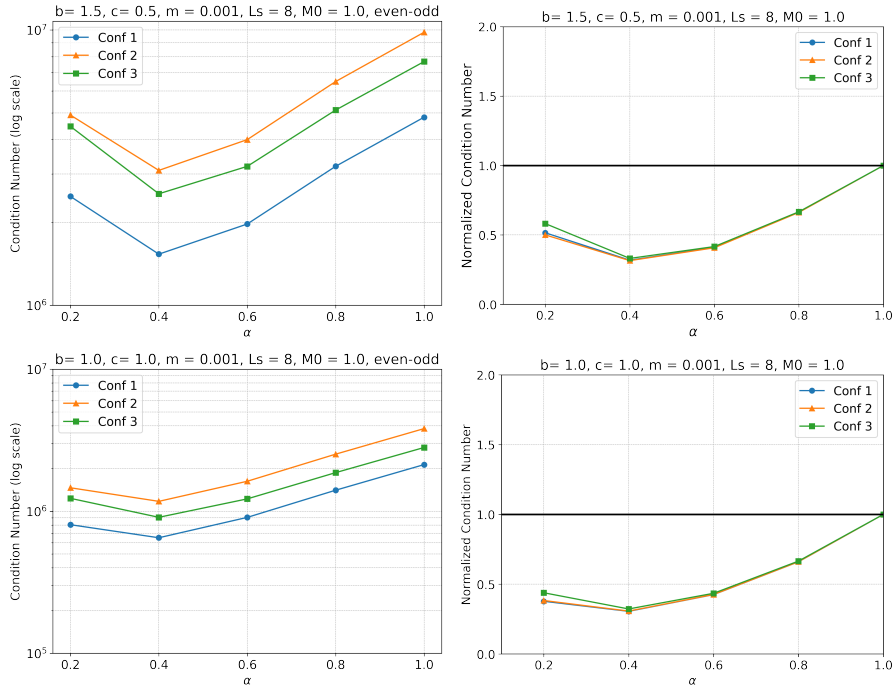


Fig. 4. Result of the condition number on the 16^4 lattice at $\beta = 6.0$ for the domain-wall operator with link smearing with parameters $M_0 = 1.0$, $(b, c) = (1.5, 0.5)$ (top panels) and $(1.0, 1.0)$ (bottom), $m = 0.001$. The left panels show the observed condition number on three configurations. The right panels show the condition numbers normalized by the values for $\alpha = 1$.

In the context of this paper, we focus on the effect of α on the convergence number of iterations. As Figure 5 shows, the optimal values of α are almost unchanged from those on the 16^4 lattice at the same β with similar improving rates. This result implies that incorporating α in the domain-wall operator results in improved convergence of the even-odd preconditioned CG solver almost independently of lattice volume.

3.4 Result for $\beta = 5.7$ on the 16^4 lattice

We also examine a 16^4 lattice with configurations generated at $\beta = 5.7$, which roughly corresponds to the lattice spacing $a \simeq 0.2$ fm. This implies that the physical volume is almost the same as that of 32^4 lattice at $\beta = 6.0$. We adopt the same values of the quark mass m in lattice units as those for $\beta = 6.0$, which means that the mass in physical units is halved correspondingly.

Figure 6 shows that the α improvement effect diminishes as the quark mass becomes larger. Similar to the case of $\beta = 6.0$, the optimal improvement is

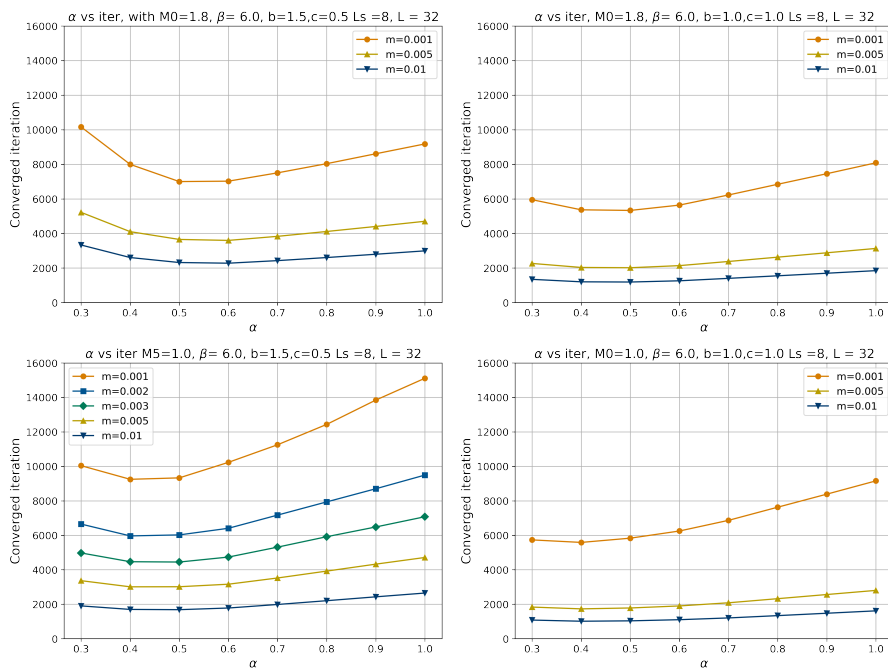


Fig. 5. Converged numbers of CG iterations on 32^4 lattice at $\beta = 6.0$. Top panels show $M_0 = 1.8$ (without smearing), $(b, c) = (1.5, 0.5)$ (left) and $(b, c) = (1.0, 1.0)$ (right). Bottom panels show $M_0 = 1.0$ (with smearing), $(b, c) = (1.5, 0.5)$ (left) and $(b, c) = (1.0, 1.0)$ (right). In both cases, $L_s = 8$ is used.

observed when α is in the range of 0.4 to 0.5. The acceleration of CG convergence for $m = 0.001$ is in the range of 20% (top-left panel)–30% (top-left).

4 Conclusion and outlook

In this paper, we examined the effect of the improved form of the domain-wall fermion operator on the convergence of the linear equation solver. In a wide range of parameters, this form indeed improves the convergence of the even-odd preconditioned CG solver by about several tens of percent, in the range of 20-40% for our smallest value of the quark mass. The required modification of the simulation code is small and the increase in the arithmetic operations is negligible compared to the observed gain. Indeed, in a modern simulation environment where the memory bandwidth or communication overhead is more relevant to the performance than the arithmetic operations, this modification has little effect on the simulation time. Thus the practical use of the improved form of the domain-wall fermion matrix is highly attractive.

In a future release, the Bridge++ code set will incorporate the improved form as the standard implementation of the domain-wall fermion matrix.

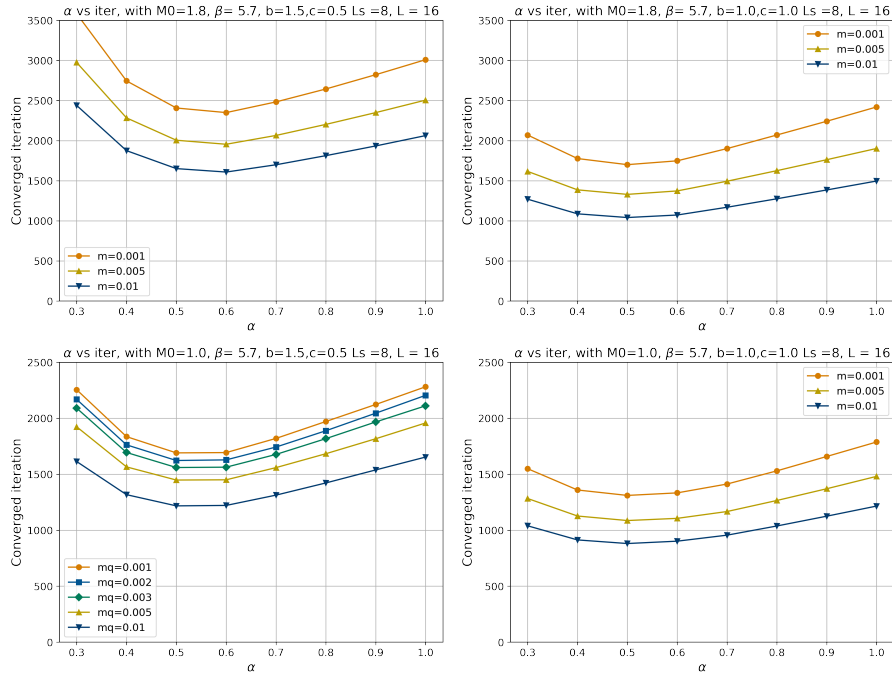


Fig. 6. Converged numbers of CG iterations on 16^4 lattice at $\beta = 5.7$. Top panels show $M_0 = 1.8$ (without smearing), $(b, c) = (1.5, 0.5)$ (left) and $(b, c) = (1.0, 1.0)$ (right). Bottom panels show $M_0 = 1.0$ (with smearing), $(b, c) = (1.5, 0.5)$ (left) and $(b, c) = (1.0, 1.0)$ (right). In both cases, $L_s = 8$ is used.

Acknowledgment

We thank the members of the Bridge++ project for useful discussions. The code development and measurement were performed on the Cygnus and Pegasus systems at University of Tsukuba and Wisteria/BDEC-01 at University of Tokyo through the Multidisciplinary Cooperative Research Program in Center for Computational Sciences, University of Tsukuba. The code development was also done on the Supercomputer Fugaku (through Usability Research ra000001) at RIKEN Center for Computational Science. This work is supported by JSPS KAKENHI (JP20K03961, JP22H00138, JP23K22495), MEXT as “Program for Promoting Researches on the Supercomputer Fugaku” (Simulation for basic science: approaching the new quantum era, PMXP1020230411) and Joint Institute for Computational Fundamental Science (JICFuS).

References

1. Akahoshi, Y., Aoki, S., Aoyama, T., Kanamori, I., Kanaya, K., Matsufuru, H., Namekawa, Y., Nemura, H., Taniguchi, Y.: General purpose lattice QCD code

- set Bridge++ 2.0 for high performance computing. *J. Phys. Conf. Ser.* **2207**(1), 012053 (2022). <https://doi.org/10.1088/1742-6596/2207/1/012053>
2. Arthur, R., et al.: Domain Wall QCD with Near-Physical Pions. *Phys. Rev. D* **87**, 094514 (2013). <https://doi.org/10.1103/PhysRevD.87.094514>
 3. Borici, A.: Truncated overlap fermions: The Link between overlap and domain wall fermions. *NATO Sci. Ser. C* **553**, 41–52 (2000)
 4. Bridge++ project: Lattice QCD code Bridge++. <https://bridge.kek.jp/Lattice-code/> (2012-)
 5. Brower, R.C., Neff, H., Orginos, K.: The Möbius domain wall fermion algorithm. *Comput. Phys. Commun.* **220**, 1–19 (2017). <https://doi.org/10.1016/j.cpc.2017.01.024>
 6. Brower, R.C., Neff, H., Orginos, K.: Möbius fermions: Improved domain wall chiral fermions. *Nucl. Phys. B Proc. Suppl.* **140**, 686–688 (2005). <https://doi.org/10.1016/j.nuclphysbps.2004.11.180>
 7. Chen, W.L., Kanamori, I., Matsufuru, H.: Lattice QCD code on GPUs: Implementation and performance comparison with OpenACC and CUDA. In: Proceedings of the International Conference on High Performance Computing in Asia-Pacific Region. p. 80–89. HPCASIA '25, Association for Computing Machinery, New York, NY, USA (2025). <https://doi.org/10.1145/3712031.3712327>
 8. Chiu, T.W.: Optimal domain wall fermions. *Phys. Rev. Lett.* **90**, 071601 (2003). <https://doi.org/10.1103/PhysRevLett.90.071601>
 9. Colquhoun, B., Hashimoto, S., Kaneko, T., Koponen, J.: Form factors of $B \rightarrow \pi \ell \nu$ and a determination of $|V_{ub}|$ with Möbius domain-wall fermions. *Phys. Rev. D* **106**(5), 054502 (2022). <https://doi.org/10.1103/PhysRevD.106.054502>
 10. Furman, V., Shamir, Y.: Axial symmetries in lattice QCD with Kaplan fermions. *Nucl. Phys. B* **439**, 54–78 (1995). [https://doi.org/10.1016/0550-3213\(95\)00031-M](https://doi.org/10.1016/0550-3213(95)00031-M)
 11. Ginsparg, P.H., Wilson, K.G.: A Remnant of Chiral Symmetry on the Lattice. *Phys. Rev. D* **25**, 2649 (1982). <https://doi.org/10.1103/PhysRevD.25.2649>
 12. Hasenfratz, P., Laliena, V., Niedermayer, F.: The Index theorem in QCD with a finite cutoff. *Phys. Lett. B* **427**, 125–131 (1998). [https://doi.org/10.1016/S0370-2693\(98\)00315-3](https://doi.org/10.1016/S0370-2693(98)00315-3)
 13. Kaplan, D.B.: A Method for simulating chiral fermions on the lattice. *Phys. Lett. B* **288**, 342–347 (1992). [https://doi.org/10.1016/0370-2693\(92\)91112-M](https://doi.org/10.1016/0370-2693(92)91112-M)
 14. Luscher, M.: Exact chiral symmetry on the lattice and the Ginsparg-Wilson relation. *Phys. Lett. B* **428**, 342–345 (1998). [https://doi.org/10.1016/S0370-2693\(98\)00423-7](https://doi.org/10.1016/S0370-2693(98)00423-7)
 15. Morningstar, C., Peardon, M.J.: Analytic smearing of SU(3) link variables in lattice QCD. *Phys. Rev. D* **69**, 054501 (2004). <https://doi.org/10.1103/PhysRevD.69.054501>
 16. Neff, H.: A better conditioned Domain Wall Operator (2015), 1501.04950 [hep-lat]
 17. Shamir, Y.: Chiral fermions from lattice boundaries. *Nucl. Phys. B* **406**, 90–106 (1993). [https://doi.org/10.1016/0550-3213\(93\)90162-I](https://doi.org/10.1016/0550-3213(93)90162-I)